

Research Paper

Upregulation of LRRC8A by m⁵C modification-mediated mRNA stability suppresses apoptosis and facilitates tumorigenesis in cervical cancer

Yanjie Chen^{1#}, Xinzhao Zuo^{1#}, Qinglv Wei^{1#}, Jie Xu¹, Xiaoyi Liu¹, Shiling Liu², Haocheng Wang¹, Qingya Luo³, Yuya Wang¹, Yu Yang¹, Hongyan Zhao^{1,4}, Jing Xu¹, Tao Liu^{1✉}, Ping Yi^{1✉}

1. Department of Obstetrics and Gynecology, The Third Affiliated Hospital of Chongqing Medical University, Chongqing 401120, China.
2. Department of Obstetrics and Gynecology, Daping Hospital, Army Medical University, Chongqing 400042, China.
3. Department of Pathology, Southwest Hospital, Army Medical University, Chongqing 400038, China.
4. Institute of Basic Medical Sciences, Hubei University of Medicine, Shiyan, Hubei 442000, China.

#These authors contributed equally to this work.

✉ Corresponding authors: **Ping Yi**. Address: Department of Obstetrics and Gynecology, The Third Affiliated Hospital of Chongqing Medical University, Chongqing 401120, China. E-mail: yiping@cqmu.edu.cn. **Tao Liu**. Address: Department of Obstetrics and Gynecology, The Third Affiliated Hospital of Chongqing Medical University, Chongqing 401120, China. E-mail: anti1988@163.com.

© The author(s). This is an open access article distributed under the terms of the Creative Commons Attribution License (<https://creativecommons.org/licenses/by/4.0/>). See <http://ivyspring.com/terms> for full terms and conditions.

Received: 2022.09.23; Accepted: 2022.12.13; Published: 2023.01.01

Abstract

Cervical cancer (CC) is one of the most common gynecological malignancies with poor prognosis for advanced CC patients. LRRC8A is a volume-regulated anion channel protein involved in cellular homeostasis, but its role in CC remains largely unknown. In this study, we found that LRRC8A is elevated in CC and associated with poor prognosis. LRRC8A maintains cell survivals under the hypotonic condition, and promotes tumorigenesis through apoptosis suppression *in vitro* and *in vivo*. Notably, LRRC8A is upregulated by NSUN2-mediated m⁵C modification. m⁵C modified-LRRC8A mRNA is bound by the RNA binding protein YBX1 followed by the increased RNA stability. Moreover, loss of NSUN2 suppresses the proliferation and metastasis of CC cells, and NSUN2 expression is positively correlated with LRRC8A expression in CC. Altogether, our study demonstrates that the NSUN2-m⁵C-LRRC8A axis is crucial and would be a potential therapeutic target for CC.

Introduction

Cervical cancer (CC) is one of the most common gynecological malignancies throughout the world and has emerged as a prominent public health focus. According to the statistics in 2020, there are over 600,000 new cases and 340,000 deaths globally each year [1-3]. Persistent infection of high-risk human papillomavirus (HPV) causes the majority of CC, thus making it a rare preventable cancer. It can be prevented through HPV vaccination and treatment with surgical therapy, chemotherapy, and radiotherapy. However, there is still a high proportion of advanced CC at initial diagnosis with 52% of cases with regional involvement or distant metastasis, resulting in the poor prognosis of patients with

advanced CC [4]. Therefore, CC remains a great medical challenge and requires new potential targets.

Maintenance of a relatively constant cell volume is the critical cell function to keep cellular homeostasis. Cell proliferation and apoptosis are associated with normotonic alterations of cell volume [5, 6]. The variation of osmotic pressures is a crucial factor to result in cell volume regulation [7]. Extracellular hyposmolality or intracellular hyperosmosis induces cell swelling, and osmotically swollen cells restore their original volume and protect themselves via a process called regulatory volume decrease (RVD) [8]. LRRC8A was recently identified as an essential component of the volume-regulated

anion channel (VRAC) which is activated when a cell swelling [9]. VRAC plays an essential role in RVD process, and LRRC8A was the core functional component of VRAC [10]. LRRC8A can promote the proliferation and migration of cancer cells in a variety of cancers [11]. In hepatocellular carcinoma and gastric cancer, LRRC8A was highly expressed, and knockdown of LRRC8A significantly inhibited cell proliferation and migration, and induced apoptosis, suggesting that the constant cell volume might be involved in the malignancy of tumors [12, 13].

Recently, the association between abnormal RNA modifications and tumorigenesis has attracted widespread attention [14]. The 5-methylcytosine (m⁵C) RNA modification, as an abundant modification, plays an important role in RNA metabolic processes, such as RNA stability, RNA processing, RNA export, and mRNA translation [15-20]. Dysregulation of m⁵C modification has been linked to various diseases including cancer [21]. In bladder cancer, m⁵C deposited in 3' UTR of heparin binding growth factor (HDGF) mRNA enhances its stability, and therefore exhibits the essential oncogenic role [16]. LIN28B binds to m⁵C-modified GRB2 mRNA, promotes its expression, and ultimately activates PI3K/AKT and ERK/MAPK oncogenic signaling pathways in esophageal squamous cell carcinoma [17]. m⁵C modification exists in 94% of mRNA in HeLa cells, indicating that the regulation of RNA fate by m⁵C modification may be an important mechanism leading to the occurrence and development of cervical cancer. However, whether or not the m⁵C modification affects tumorigenesis by regulating cell homeostasis is little known.

Our results revealed that LRRC8A mRNA is subjected to m⁵C modification and upregulated in CC cells. Higher expression of LRRC8A predicts poor prognosis for CC patients. Depletion of LRRC8A induces apoptosis under the hypotonic condition and suppresses tumorigenesis of CC cells. The m⁵C methyltransferase NSUN2 mediates m⁵C modification of LRRC8A mRNA and increases its stability. Our study demonstrates that the NSUN2-m⁵C-LRRC8A axis is crucial for tumorigenesis of CC.

Materials and methods

Cervical tumor samples and cell culture

All cervical squamous cell carcinoma and normal cervical tissue specimens were obtained from patients undergoing surgery in Daping Hospital of the Army Military Medical University from 2020-03-01 to 2020-05-30. All subjects were informed the consent, and all these specimens were pathologically verified and reviewed by the institutional board of the

Third Affiliated Hospital of Chongqing Medical University (2022033). HEK293T and HeLa cells were cultured in Dulbecco's Modified Eagle's medium (DMEM) high glucose medium (GIBCO, USA), and SiHa cells were cultured in minimum Eagle's medium (MEM) (GIBCO, USA). Medium was supplemented with 10% fetal bovine serum (FBS) (GIBCO, USA) and 1% penicillin-streptomycin (Solarbio, China), and cells were incubated at 37°C with 5% CO₂ in a humidified atmosphere. Cells where indicated were treated with the AKT phosphorylation agonist SC79 (MedChemExpress, USA).

Plasmids, cell transfection, and lentiviral infection

For LRRC8A and NSUN2 knockdown, all shRNAs including shCtrl (scramble), sh1 and sh2 were cloned into pLKO.1 backbone with puromycin selection. The related sequences of shRNAs were shown in the supplementary table. For LRRC8A overexpression, full-length LRRC8A coding sequence was cloned into pCDNA3.1 vector (Youbio). Overexpression of NSUN2 was conducted by the full-length NSUN2 coding sequence cloned into pCDH vector (Addgene). NSUN2-WT and NSUN2-MUT (C271, C321) expression plasmids were constructed by using the pEnter vector (Addgene), and the empty vector was used as the negative control.

Plasmid transfection was conducted by using jetPRIME transfection (Polyplus, France). After 24 hours or later, the levels of mRNA and protein were measured. Lentiviral vectors were transfected into HEK293T cells with packaging vectors psPAX2 (#12260, Addgene) and pMD2.G (#12259, Addgene) by using jetPRIME transfection (Polyplus, France). Infectious lentivirus particles were harvested at 48 hours after transfection.

Quantitative reverse transcription-polymerase chain reaction (qRT-PCR)

Trizol reagent (Sigma, USA) was used to extract total RNA from HeLa cells and SiHa cells. For mRNA expression analysis, qRT-PCR was performed by using SYBR Green Master Mix (Vazyme) on QuantStudioDx instrument (Life Technologies). A typical cycling condition included 95°C for 5 min followed by 40 cycles at 95°C for 10 s, 60°C for 30 s. GAPDH was used as the internal standard control. Each sample runs in triplicate. Primers used in qRT-PCR were listed in the supplementary table.

Western blot

HeLa and SiHa cells were treated with lysis buffer containing protease inhibitors (APEX BIO, USA) for western blot and IP (Beyotime, China). Cells were

lysed on ice for 30 min, and the lysate was obtained by centrifugation at 12,000 rpm for 15 min. The concentration of proteins was measured by using a bicinchoninic acid BCA protein assay kit (Solarbio, China). Then the proteins were resolved by 10% SDS-PAGE and transferred on PVDF membranes (Millipore, USA). The membrane was blocked with 5% non-fat milk in TBS/Tween-20 for 1 hour at room temperature. After blocking, the membranes were blotted with primary antibodies against LRRC8A (24979S, CST, 1:1000), NSUN2 (20854-1-AP, Proteintech, 1:2000), Flag-tag (20543-1-AP, Proteintech, 1:2000), YBX1 (7944S, CST, 1:1000), Caspase-3 (9662S, CST, 1:1000), p-AKT (4060S, CST, 1:1000), AKT (60203-2-Ig, Proteintech, 1:1000), p-PI3K (CY6428, 1:500, Abways), PI3K (#4249, 1:1000, CST), or GAPDH (60004-1-Ig, Proteintech, 1:1000) overnight at 4°C. After being washed with TBS/Tween-20, the PVDF membranes were incubated with chemiluminescent secondary antibody (SA00001-1/SA00001-2, Proteintech, 1:10000).

Immunohistochemistry (IHC)

After dewaxing the paraffin sections of tissues, heat induced antigen retrieval was conducted. The slides were blocked with goat serum (ZSGB-BIO, ZLI-9021) at 37°C for 30 min, and then incubated with primary antibodies against LRRC8A (17155-1-AP, Proteintech, 1:50), NSUN2 (20543-1-AP, Proteintech, 1:100), Caspase-3 (9662S, CST, 1:100), Ki67 (AF0198, Affinity, 1:100) at 4°C overnight. On the next day, the slides were incubated with the biotinylated secondary antibody at room temperature for 45 min, and then subjected to the DAB kit (ZSGB-BIO, ZLI-9018). The sections were stained with hematoxylin, decolorized with hydrochloric acid and ethanol, dehydrated and then mounted. The comprehensive score of immunostaining was evaluated independently by two professional pathologists.

Cell proliferation and cell growth analyses

For cell proliferation assay, 1500 HeLa or 2500 SiHa cells were planted in 96-well plates with 200 μ l fresh medium. Cell viabilities were measured after adding Cell Counting Kit-8 (CCK-8, Dojindo, Japan) for 2 hours. The stably transfected cells were plated into 96-well plates and incubated at 37°C for 6 hours until adherence and were referred to as 0 hour. Cell numbers were counted on 24, 48, 72, 96 hours. For the colony formation assay, transfected cells were seeded into 6-well plates. HeLa cells were plated with 1500 cells per well, and SiHa cells were plated with 2500 cells per well with 2 ml fresh medium and grown for 2 weeks. The colonies were fixed with 4% paraformaldehyde. After stained with crystal violet,

the visible colonies were counted.

Apoptosis assay

HeLa or SiHa cells were incubated with Annexin V and PI (DOJINDO, Japan) according to the instructions given by the manufacturer. The stained cells were subjected to flow cytometry. BD Accuri C6 flow cytometer (BD Biosciences, USA) was used to analyze apoptosis and the percentage of Annexin V+ PI- and Annexin V+ PI+ cells was calculated as the apoptosis rate.

Cell migration and invasion assays

Migration and invasion assays were performed by using transwell chambers (8 μ m, Corning Falcon). Stably transfected cells (HeLa, 6×10^4 ; SiHa, 8×10^4) and 250 μ l serum-free medium were all added into the upper chamber of a transwell coated with or without Matrigel (Corning Incorporated, USA). The lower chamber was added with 650 μ l cell culture medium containing 10% FBS. After incubation for 24 hours, the chambers were collected and stained by 0.5% crystal violet. The cells passing through the membrane were counted in three random fields.

Cell swelling assays

For observing single cell morphological changes, stably transfected cells were planted in 12-well plates with 1 ml fresh medium for 6 hours until adherence. Then medium was changed into ddH₂O and were referred to as 0 min. Morphological changes were assessed using an optical microscope. For cells that survived after swelling, 8000 HeLa and SiHa cells were treated in ddH₂O for 0, 5, 10 min/0, 10, 20 min. Then cells were planted in 96-well plates with 200 μ l fresh medium. After cells adherence, cell viabilities were measured after incubation with CCK-8 for 2 hours.

Xenograft model in nude mice

Stably transfected HeLa cells (2×10^7 cells) were injected subcutaneously into the thigh of BALB/c nude mice (4-6 weeks old, 5 mice/group). The length and width of the subcutaneous tumor was measured every 3 or 4 days. After injection for 22 or 24 days, the mice were euthanized, and the tumor weight was measured. The tumors were isolated and fixed in 4% formalin for IHC analysis. Animal studies were approved by the Ethics Committee of the Third Affiliated Hospital of Chongqing Medical University (2022033).

RNA m⁵C dot blot

mRNA was purified by mRNA Isolation System IV kit (Poly Tract, USA). The m⁵C dot blot was performed on Amersham Hybond-N+ membrane (GE

Healthcare, UK). After cross-linked by ultraviolet and blocked by PBST+5% milk for 1 hour, the membranes were incubated with the primary antibody against m⁵C (ab214727, Abcam, 1 µg/ml) overnight at 4°C. On the next day, the membrane was washed 3 times with PBST, and incubated with the secondary anti-rabbit antibody for 1 hour. Then the membrane was washed again with PBST. Finally, we used the chemiluminescence system to visualize the membrane. RNA levels were normalized with methylene blue staining to ensure consistency.

RNA-sequencing (RNA-seq)

Total RNA was isolated using TRIzol Reagent (Sigma, USA). cDNA libraries were constructed by using NEBNext Ultra RNA Library Prep Kit for Illumina (New England BioLabs). All samples were sequenced on illumina Nova platform. Using STAR version 2.7.8a, all the clean reads were aligned to homo sapiens GENCODE GRCh38.v35 and counted the reads by featureCounts version 2.0.3. R package DESeq2 was used for differential expressed genes identification.

RNA immunoprecipitation (RIP) assay

About 2×10^7 HeLa cells or 4×10^7 SiHa were lysed in RIP lysis buffer (HEPES 20 mM, 150 mM NaCl, 10 mM KCl, 5 mM EDTA, 5 mM MgCl₂, 0.5% NP40, 10% glycerol). After incubation for 30 minutes on the ice, the lysate was harvested by centrifugation at 12,000 rpm for 10 min. The specific antibody (3 µg) or control IgG (3 µg) was incubated with the supernatant lysate overnight at 4°C. Next day, Dynabeads Protein A beads (Invitrogen, USA) were added into the lysate and incubated at 4°C for 3 hours. After washed three times with RIP lysis buffer, the co-precipitated RNA was extracted with Trizol Reagent (Sigma, USA). RNA was isolated and RT-qPCR was performed as described previously.

Methylated RNA immunoprecipitation (MeRIP) assay

Total RNA was extracted by Trizol reagent (Sigma, USA) and then treated with RNase-free DNase set. After immunoprecipitated with anti-m⁵C antibody (3 µg/ml), Dynabeads Protein A beads (Invitrogen, USA) were added and incubated at 4°C for 3 hours. After washes, RNA was isolated, and RT-qPCR was performed as described previously.

RNA stability assay

To test RNA stability, transfected HeLa or SiHa cells were seeded into 12-well plates. 5 µg/ml of actinomycin D (AbMole, USA) was added into each well and incubated for 0, 2, 4, 6 hours. Total RNA was extracted at the indicated time, and mRNA level was

analyzed by qRT-PCR.

Statistical analysis

All continuous data were shown as the mean \pm SD and the significance of differences was evaluated by two tailed t-tests between two groups. It is considered statistical significant when $p < 0.05$, and in all cases, the p values were remarked as follows: *** $P < 0.001$, ** $P < 0.01$, * $P < 0.05$, but statistically insignificant when $P > 0.05$. The growth rates difference was determined by ANOVA with repeated measures analysis of variances. The correlation between LRRC8A and NSUN2 expression in cervical cancer was analyzed by Spearman rank correlation analysis. All statistical analyses were performed using Graphpad Prism 8.

Results

LRRC8A is highly expressed and acts as a poor prognostic factor in CC

We firstly analyzed the mRNA levels of LRRC8 subunits (LRRC8A-E) [22-24] in CC tissues compared with normal tissues by using two GEO datasets (GSE63514 and GSE52904) and found that LRRC8A and LRRC8B were upregulated in CC tissues (Fig. 1A, B, Fig. S1A, B). We also observed the aberrantly overexpression of LRRC8A in CC in the Biewenga Cervix dataset according to the Oncomine database (Fig. 1C). Consistent with this, IHC assays showed that the protein abundance of LRRC8A was elevated in CC tumors when compared with normal cervix uteri tissues (Fig. 1D, E). Furthermore, we analyzed the survivals of CC patients with distinct expression of LRRC8 subunits by Kaplan-Meier survival analysis [25,26]. Patients with higher LRRC8A expression had shorter recurrence free survival (RFS) time (Fig. 1F). However, the RNA levels of LRRC8B-E were not associated with of patients' RFS (Fig. S1C). Taken together, these data indicate that LRRC8A is frequently upregulated in CC and predicts poor prognosis for CC patients.

LRRC8A promotes tumorigenesis of CC *in vitro* and *in vivo*

To explore the role of LRRC8A in CC cells, LRRC8A was overexpressed in HeLa and SiHa cells, and its effect on cell growth, migration and invasion was detected (Fig. 2A). CCK-8 and colony formation assays showed that LRRC8A overexpression resulted in enhanced cell growth. Transwell assays demonstrated that LRRC8A overexpression significantly increased the migration and invasion capabilities of CC cells (Fig. 2B-E). To further confirm the oncogenic effect of LRRC8A in CC cells, we constructed lentivirus-mediated LRRC8A knockdown HeLa cells

and SiHa cells (Fig. 2F). As expected, reduced LRRC8A expression inhibited the proliferation, migration, and invasion of HeLa and SiHa cells (Fig. 2G-J). Moreover, subcutaneous tumorigenesis model was applied to assess the function of LRRC8A in CC *in vivo*. Compared with control group, xenograft tumors obtained from mice which burdened cells with LRRC8A knockdown were smaller and lighter (Fig. 2K-M, Fig. S2A). Together, these results demonstrate that LRRC8A facilitates tumorigenesis of CC *in vitro* and *in vivo*.

LRRC8A keeps cellular homeostasis in CC cells

LRRC8A is an essential component of VRAC, a complex which is indispensable for homeostasis by resisting cell swelling. Cell size and cell deformability represent two key biophysical attributes of cells that have been demonstrated to modulate cancer invasion and metastasis [27]. Thus, we detected whether LRRC8A was involved in maintaining cellular homeostasis in CC cells under hypotonic conditions. Under the optical microscope, we observed that LRRC8A-overexpressed cells remained constant both in volume and cell morphology compared with the control CC cells with slightly larger gradually under hypotonic conditions. Conversely, LRRC8A

knockdown accelerated swelling and broken of CC cells upon hypotonic solution treatment (Fig. 3A, B). We also measured the cell viability after treatment with hypotonic solution at different time points by CCK-8 assays. Results showed that compared with control group, LRRC8A overexpression promoted the cell survival after hypotonic solution treatment, but LRRC8A depletion significantly decreased the cell survival (Fig. 3C, D). Consistently, Annexin V/DAPI staining showed that depletion of LRRC8A results in increased apoptosis of CC cells, demonstrated that LRRC8A might promote survivals of CC cells through inhibiting apoptosis (Fig. S2B, C). Moreover, chemotherapy sensitivity assays revealed that CC cells with LRRC8A knockdown had higher sensitivity to cisplatin (Fig. S2D). These results suggested that LRRC8A might confer chemotherapy resistance in CC. PI3K/AKT, the essential signaling pathway associated with cell apoptosis and proliferation, has been reported regulated by LRRC8A [11,28,29,33]. LRRC8A knockdown could reduce reactive oxygen species generation, resulting in the inactivation of PI3K/AKT signaling [30]. LRRC8A-driven AKT phosphorylation can be inhibited by LY294002 (a PI3K phosphorylation inhibitor) [33]. Consequently, we explored the effect of LRRC8A on the PI3K-AKT signaling pathway in CC cells, and the outcomes

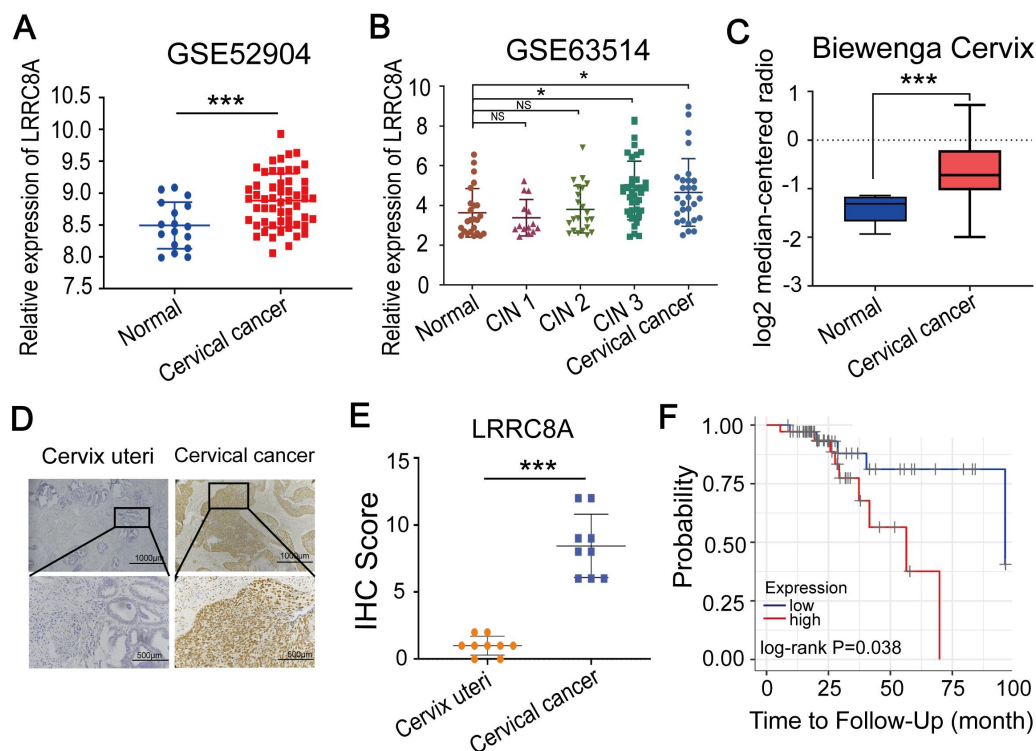


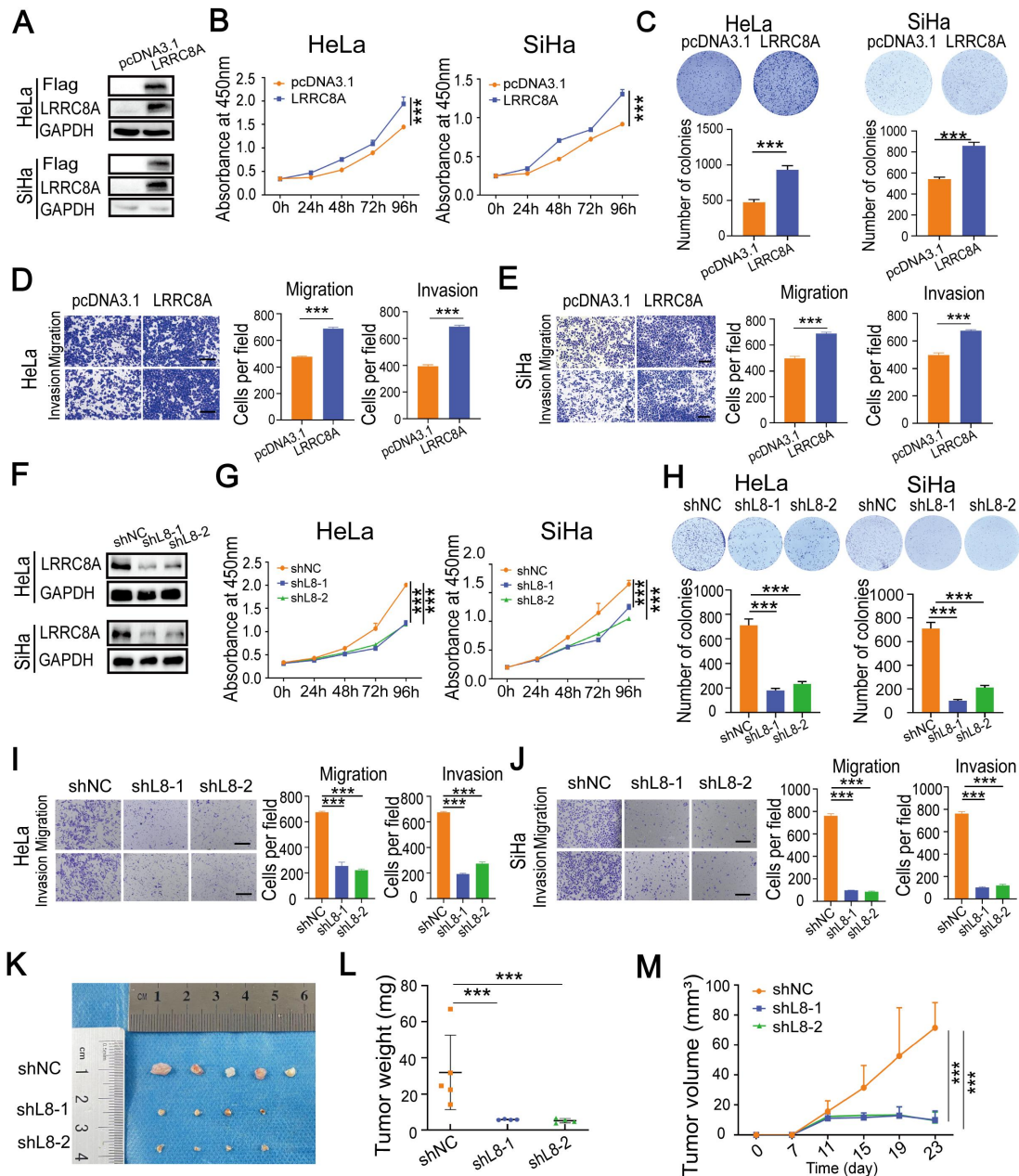
Figure 1. Elevated expression of LRRC8A in CC predicts poor prognosis. (A, B) Relative RNA levels of LRRC8A in CC tissues and normal cervical epithelium in GEO datasets. **(C)** Relative RNA levels of LRRC8A in CC tissues and cervix uteri in Oncomine database. **(D)** Representative IHC staining images of LRRC8A protein levels in CC tissues and cervical epithelium tissues. Scale bar, upper: 100 μ m, lower: 500 μ m. **(E)** The quantitative analysis of LRRC8A protein expression in CC tissues and cervical epithelium tissues assessed by IHC staining. **(F)** Kaplan-Meier analysis of CC patients' RFS based on LRRC8A expression by TIMER website. * $P < 0.05$, ** $P < 0.01$, *** $P < 0.001$, NS, not significant.

showed that LRRC8A knockdown inhibited PI3K-AKT signaling activation and promoted the expression of Caspase-3 in CC cells (Fig. 3E). In addition, the intervention of SC79 (an AKT phosphorylation agonist) could significantly rescue the suppression of AKT phosphorylation by LRRC8A knockdown (Fig. 3F). Furthermore, SC79 treatment improved the growth rate of cells with LRRC8A knockdown (Fig. S2E, F). Transwell assays exhibited that activation of AKT signaling by SC79 rescued the cell mobility of CC cells with LRRC8A knockdown

(Fig. S2G).

LRRC8A upregulation by m⁵C RNA methyltransferase NSUN2 in CC

A recent RNA-BisSeq analysis described that LRRC8A might be regulated by m⁵C modification [31]. To explore the relationship between LRRC8A and m⁵C modification, we performed meRIP-PCR by using an antibody specific to m⁵C within RNAs in CC cells. Results showed that LRRC8A was subjected to m⁵C modification and knockdown of the m⁵C



methyltransferase NSUN2 could decrease the m⁵C modification of LRRRC8A mRNA (Fig. 4A). Consistently, dot blot assays showed that NSUN2 knockdown decreased the global m⁵C level of mRNAs in both CC cells (Fig. 4B). Then we conducted RNA-seq upon NSUN2 knockdown and RIP-seq of NSUN2 to further study m⁵C-mediated gene regulation in CC cells. 1669 downregulated and 1251 upregulated genes in HeLa cells, and 1064 downregulated and 734 upregulated genes in SiHa cells were identified upon NSUN2 knockdown (Fig. 4C, Fig. S3A, B). Using gene ontology analysis, pathways enriched by these altered genes were essential for tumorigenesis such as PI3K-Akt signaling pathway (Fig. 4D). Meanwhile, NSUN2 bound 4390 transcripts by RIP-seq of NSUN2 in SiHa

cells (Fig. 4E). Through overlapping these omics data, we found 30 transcripts, including LRRRC8A, were m⁵C modified, bound by NSUN2 and differentially expressed after NSUN2 knockdown in both HeLa and SiHa cells (Fig. 4F). Furthermore, the common motifs including the m⁵C motif was found in these 30 transcripts targeted by NSUN2 (Fig. 4G), which was consistent with the previous study [31]. We further confirmed LRRRC8A regulation by NUSN2 by qRT-PCR and western blot assays. As expected, NSUN2 inhibition remarkably downregulated the RNA and protein levels of LRRRC8A in CC cells (Fig. 4H, I). Results of RIP-PCR in HeLa and SiHa cells also revealed that NSUN2 bound to LRRRC8A mRNA (Fig. 4J). Taken together, these data indicate that LRRRC8A is upregulated by the m⁵C methyltransferase NSUN2.

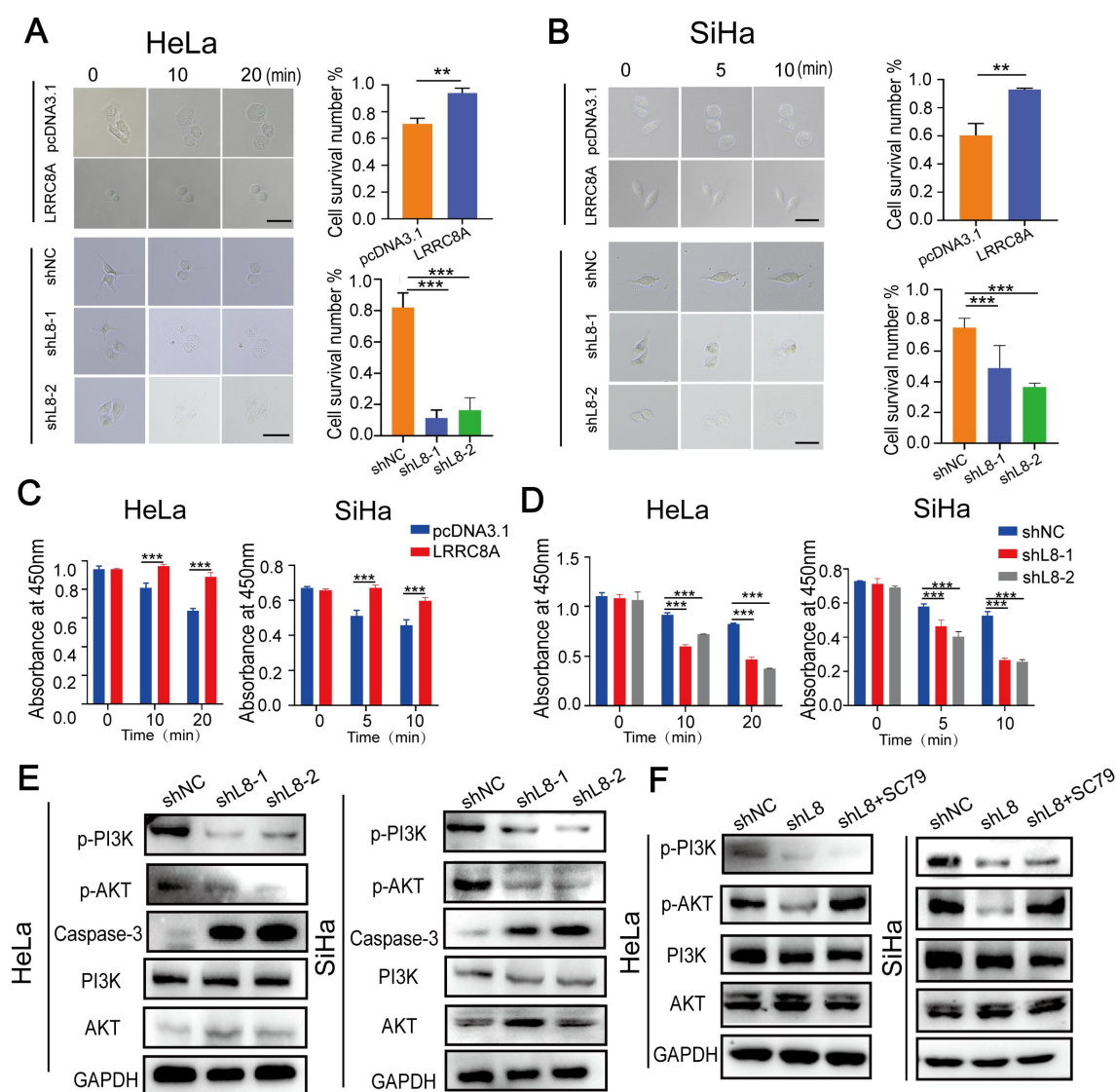


Figure 3. LRRRC8A maintains cellular homeostasis of CC cells under the hypotonic condition. (A, B) Swelling analysis of CC cells with LRRRC8A overexpression or knockdown under the the hypotonic condition. Scale bar, 10 μ m. **(C, D)** CCK-8 assays detecting the survivals of CC cells with LRRRC8A overexpression or knockdown upon the hypotonic treatment. **(E)** Changes of protein levels of p-PI3K p-AKT, PI3K, AKT and Caspase-3 in HeLa and SiHa cells upon LRRRC8A knockdown. **(F)** Protein levels of p-PI3K, p-AKT, PI3K, AKT and in LRRRC8A-depleted CC cells with or without SC79 treatment. Data are presented as means \pm S.D. **P < 0.01, ***P < 0.001.

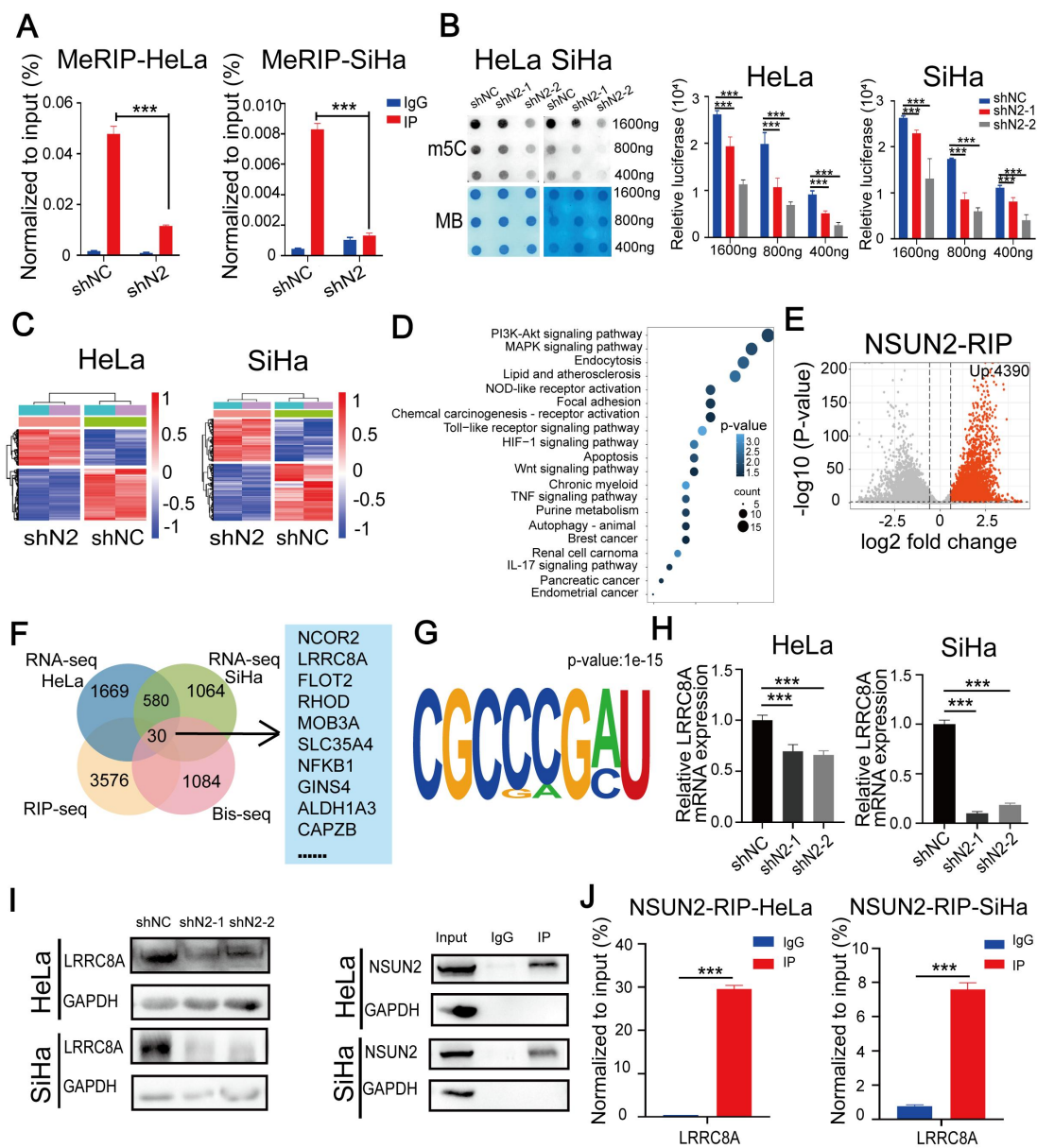


Figure 4. NSUN2 promotes m⁵C modification and expression of LRRC8A mRNA. (A) meRIP-PCR assays detecting the RNA m⁵C modification of LRRC8A in HeLa and SiHa cells upon NSUN2 knockdown. (B) Dot blot detecting the global m⁵C modification of mRNAs in CC cells with or without NSUN2 knockdown. Methylene blue (MB) staining was used as a loading control. (C) Heatmap of differentially expressed genes from RNA-seq analysis of HeLa and SiHa cells upon NSUN2 knockdown. (D) Gene ontology analysis of differentially expressed genes described in (C). (E) Volcano plot of NSUN2 bound transcripts from RIP-seq analysis in SiHa cells. (F) A Venn diagram shows the potential targets of NSUN2 through the combined analysis of RNA-seq, RIP-seq from the present study and the reported RNA Bis-seq in HeLa cells. (G) Sequence frequency logo for the sequences proximal to mRNA m⁵C sites on the 30 NSUN2-bound mRNA. (H, I) The RNA and protein levels of LRRC8A in CC cells upon NSUN2 knockdown were measured. (J) RIP-PCR assays detecting the interaction between NSUN2 and LRRC8A mRNAs in HeLa and SiHa cells. IgG was used as an internal control. GAPDH was used as the negative control in western blot assays. Data are presented as means ± S.D. ***P < 0.001.

NSUN2 enhances tumorigenesis of CC

Next, we investigated the role of NSUN2 in CC cells. Overexpressing NSUN2 notably promoted cell proliferation, migration and invasion (Fig. 5A-C, Fig. S4A-D). In contrast, knocking down NSUN2 substantially suppressed cell proliferation, migration, and invasion of CC cells (Fig. 5D-F, Fig. S4E-G). To explore the oncogenic role of NSUN2 *in vivo*, we conducted subcutaneous tumor formation experiments. Knockdown of NSUN2 resulted in the smaller and lighter xenograft tumors that formed in nude

mice when compared with the control group (Figure 5G-I, Fig. S4H). IHC assays showed that tumors formed by cells with NUSN2 knockdown exhibited lower Ki67 but higher Caspase-3 levels (Fig. 5J-L). What's more, the mRNA level of NSUN2 in CC tissues compared with normal tissues was significantly up-regulated (Fig. S4I-J). IHC assays showed that the protein abundance of NSUN2 was elevated in CC tumors compared with normal cervix uteri tissues (Fig. S4K-L). The survivals analysis showed that patients with higher LRRC8A expression had shorter recurrence free survival (RFS) time (Fig.

S4M). Thus, these results reveal that NSUN2 enhances tumorigenesis of CC and associated with poor prognosis.

m⁵C modification stabilizes LRRC8A mRNA in CC

To further explore the tumor-promoting role of NSUN2 dependently on m⁵C modification in CC, we constructed a wide-type NSUN2 expression plasmid (NSUN2-WT) and an m⁵C methyltransferase-mutated plasmid (NSUN2-MUT) by introducing point mutations in releasing and catalytic sites (cysteine 271 and 321) (Fig. 6A). Then, CC cells were transfected with wild-type or mutated NSUN2 (Fig. 6B). NSUN2-WT substantially promoted cell proliferation, migration and invasion. However, overexpressing

NSUN2 mutant had no obvious effects on the malignant phenotype of SiHa cells (Fig. 6C-E). The exactly alike conclusion was also validated in the HeLa cells (Fig. S5A-D). Further RIP assays showed that the NSUN2 mutation accounted for the dramatically reduced level of LRRC8A mRNA bound by NSUN2 in CC cells (Fig. S5E). NSUN2-mediated m⁵C modification was reported to regulate RNA stability [16,17], and the results of RNA-seq and RIP-seq also showed that transcripts bound by NSUN2 were more likely to be downregulated in the RNA level upon NSUN2 depletion (Fig. 6F, G). In this way, we detected the effect of NSUN2 on the half-life of LRRC8A mRNA. The results showed that knockdown of NSUN2 shortened the half-life of LRRC8A mRNA (Fig. 6H). Considering that the RNA

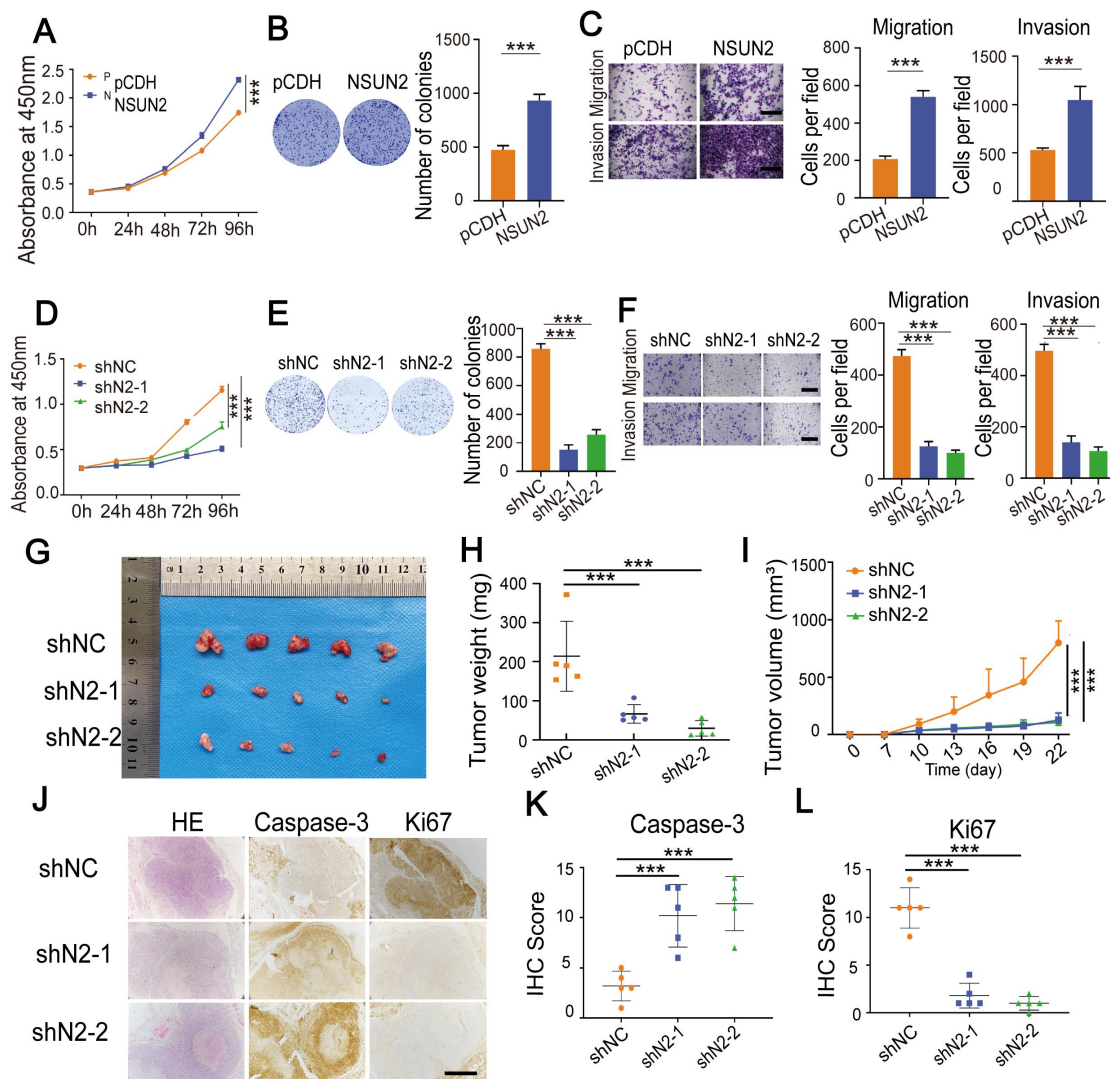


Figure 5. NSUN2 exerts a tumor-promoting role in CC. (A) CCK-8 assays showed the growth of HeLa cells upon NSUN2 overexpression. (B) The effect of NSUN2 overexpression on the colony formation of HeLa cells. (C) Transwell cell migration and invasion analysis of NSUN2 overexpressed and control HeLa cells. Scale bar, 200 μ m. (D) The effect of NSUN2 knockdown on cell growth was determined by CCK-8 assays. (E) Colony formation assays were performed in NSUN2 knockdown and control cells. (F) Migration and invasion assays of HeLa cells with or without NSUN2 knockdown. Scale bar, 200 μ m. (G-I) Effects of NSUN2 knockdown on tumor weight and volume in the subcutaneous xenograft nude mouse model. (J-L) Representative IHC staining images and quantitative analysis of Ki67 and Caspase-3 in xenograft tumors from NSUN2 knockdown and control cells treated nude mice. Scale bar, 500 μ m. Statistical analyses showed the IHC staining of Ki67 and Caspase-3 from xenograft tumors. Data are presented as means \pm S.D. ***P < 0.001.

binding protein YBX1 was involved in regulating the stability of transcripts with m⁵C modification, we investigated the influence of YBX1 on LRRC8A expression. The RT-qPCR results showed that YBX1 knockdown led to lower mRNA level of LRRC8A (Fig. 6I). RIP assays by using the antibody specific to YBX1 also showed that YBX1 accumulated LRRC8A mRNA significantly in both HeLa and SiHa cells (Fig. 6J, I). Taken together, these results indicate that NSUN2-mediated m⁵C modification stabilizes

LRRC8A mRNA.

NSUN2-LRRC8A axis is crucial for malignant growth and metastasis of CC cells

To further confirm the synergetic carcinogenic effect of LRRC8A with NSUN2 in CC, LRRC8A was re-expressed in NSUN2 knockdown cells (Fig. 7A), and the effects on cell proliferation, migration and invasion were analyzed. Ectopic expression of LRRC8A largely rescued the inhibition of

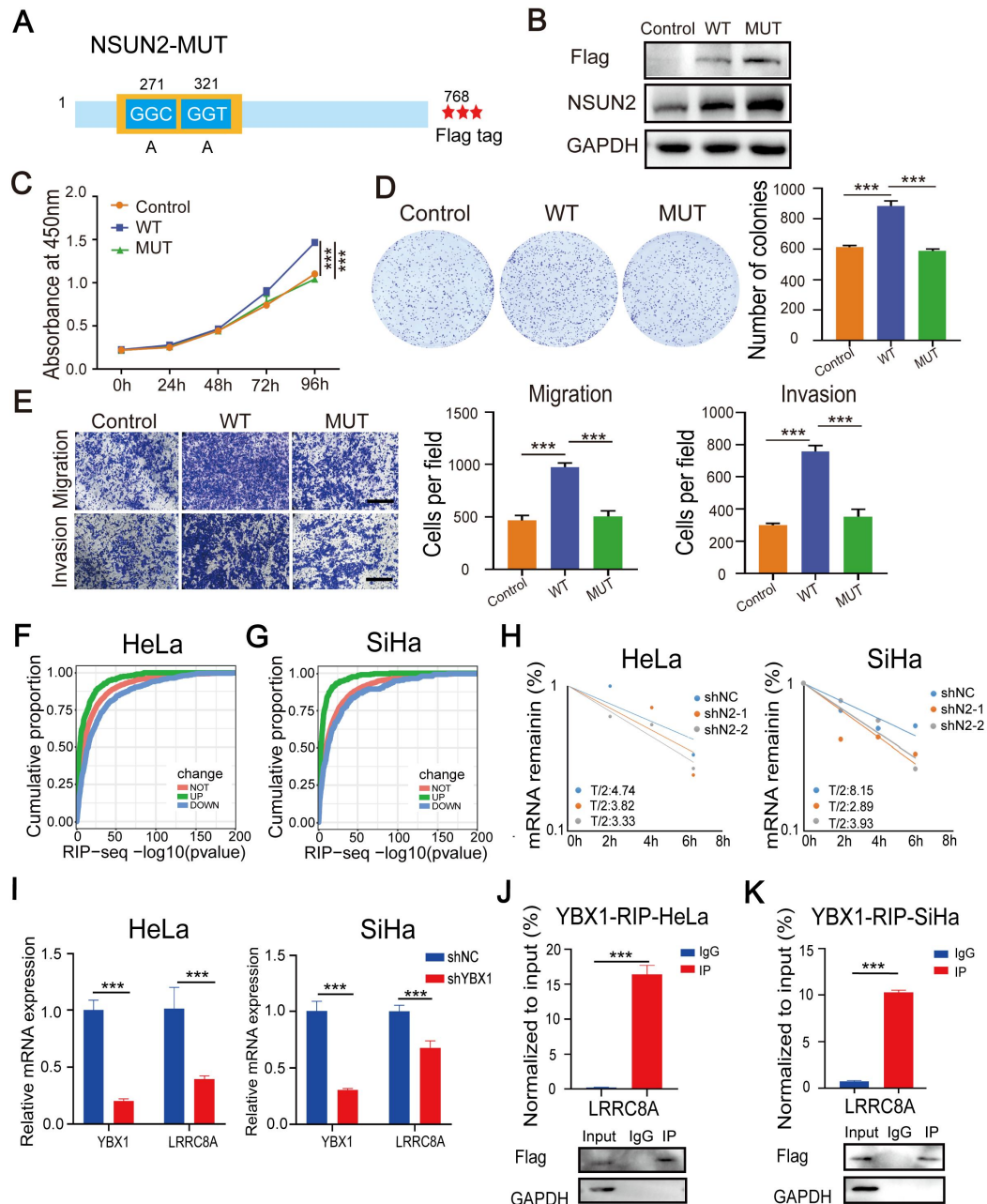


Figure 6. NSUN2 facilitates tumorigenesis of CC cells in an m⁵C-dependent manner. (A) Schematic of the NSUN2 mutant (NSUN2-MUT). (B) Western blot confirmed the overexpression of wild-type or mutated NSUN2 in CC cells. (C) CCK-8 assays of SiHa cells with forced expression of wild-type or mutated NSUN2. (D) Colony formation assays were performed in SiHa cells with forced expression of wild-type or mutated NSUN2. (E) Transwell cell migration and invasion assays of SiHa cells with NSUN2-WT and NSUN2-MUT. Scale bar, 200 μ m. (F, G) Cumulative proportion of NSUN2 bound transcripts with differentially expressed genes from RNA-seq analysis of NSUN2 knockdown in HeLa and SiHa cells. (H) Effects of NSUN2 knockdown on mRNA half-life of LRRC8A by RNA stability assays. (I, J) RT-qPCR detecting RNA levels of LRRC8A in HeLa and SiHa cells upon YBX1 knockdown. (I) RIP-PCR assays detecting the interactions between YBX1 and LRRC8A mRNA in HeLa and SiHa cells. IgG was used as an internal control. GAPDH was used as the negative control in western blot assays. Data are presented as means \pm S.D. ***P < 0.001.

proliferation rate caused by NSUN2 knockdown (Fig. 7B, C). The suppressive effect of NUSN2 knockdown on migration and invasion capacities of SiHa and HeLa cells was also partially reversed by LRRC8A restoration (Fig. 7D, E). Moreover, p-PI3K and p-AKT expression was significantly decreased with induced Caspase-3 protein level in NSUN2-depleted CC cells, and overexpressing LRRC8A could rescue PI3K-AKT signaling and inhibit Caspase-3 expression in CC cells

(Fig. 7F, Fig. S6A). In addition, the correlation analysis suggested that there was a positive correlation between the mRNA level of NSUN2 and LRRC8A in CC (Fig. 7G). In agreement with this, IHC staining exhibited that the protein expression level of and LRRC8A was remarkably declined in tumors formed by NSUN2-depleted Hela cells (Fig. 7H, I). Together, these results indicate that the NSUN2-m⁵C-LRRC8A axis is crucial for cervical tumorigenesis.

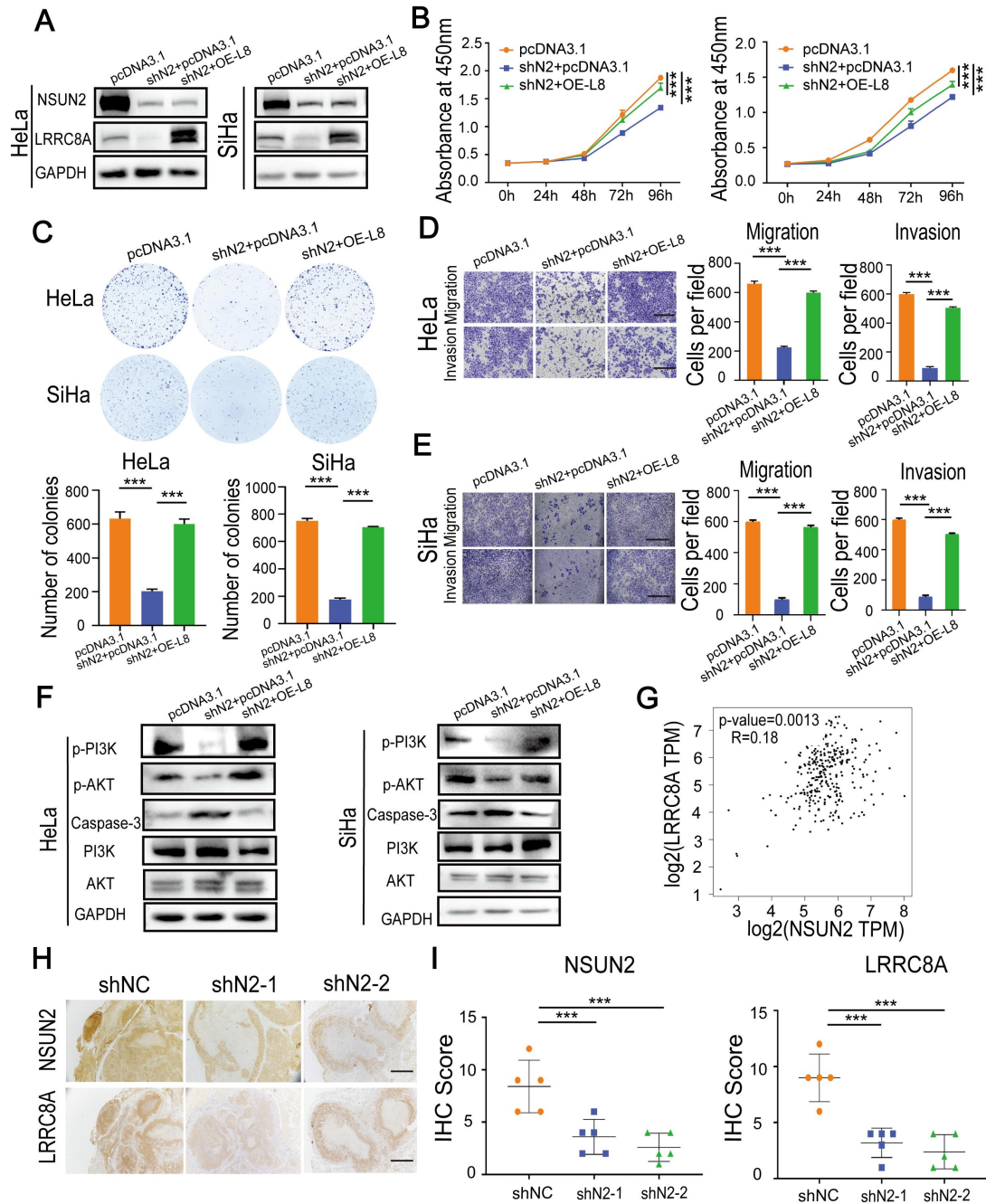


Figure 7. Overexpression of LRRC8A rescues the phenotype of CC cells with NSUN2 knockdown. (A) Western blot confirmed the protein expression of NSUN2 and LRRC8A in NSUN2-depleted CC cells with or without LRRC8A re-expression. (B) Overexpression of LRRC8A rescues the cell proliferation suppressed by NSUN2 knockdown in HeLa and SiHa cells by CCK-8 assays. (C) Overexpression of LRRC8A restores the colony formation of CC cells suppressed by NSUN2 knockdown. (D, E) Cell migration and invasion analysis of NSUN2-depleted CC cells with or without LRRC8A re-expression. Scale bar, 200 μ m. (F) Protein expression levels of p-PI3K, p-AKT, PI3K, AKT and Caspase-3 in NSUN2-depleted CC cells with or without LRRC8A re-expression. (G) Spearman's correlation analysis between mRNA levels of NSUN2 and LRRC8A in cervical cancer. (H) Representative images showing protein levels of NSUN2 and LRRC8A in nude mouse xenograft tumors. Scale bar, 500 μ m. (I) Statistical analysis of IHC score showing NSUN2 and LRRC8A levels in xenograft tumors. Data are presented as means \pm S.D. ***P < 0.001.

Discussion

LRRC8A was identified as an essential component of VRAC which plays a pivotal role in cell volume regulation [9]. It was reported that LRRC8A regulates B- and T-cell development, chemoresistance, apoptosis, small molecule transportation [12,13, 32-35]. However, limited information is currently available on the role of LRRC8A in cancer. In this study, we found that LRRC8A expression was significantly upregulated in CC and the high expression of LRRC8A was identified as a poor prognostic factor in CC. Through *in vitro* and *in vivo* experiments, we confirmed that LRRC8A depletion significantly inhibited the proliferation, migration and invasion of CC cells and promoted apoptosis.

Our results demonstrated that LRRC8A promotes tumorigenesis in CC. Consistently, LRRC8A was demonstrated to be related with growth and metastasis of hepatocellular carcinoma and gastric cancer and prognosis in colon cancer [12,13,36]. Extensive research has confirmed that cellular homeostasis regulated by various ion transporters plays a crucial role in cancers. Zinc transporters mediated signaling pathways and zinc levels lead to cancer cell proliferation and metastasis [41]. Zinc transporter SLC39A13/ZIP13 knockout depresses the malignant phenotypes of ovarian cancer cells both *in vitro* and *in vivo* [42]. Increased expression of the copper efflux transporter ATP7A mediates resistance to cisplatin, carboplatin, and oxaliplatin in ovarian cancer cells [43]. Na⁺, HCO₃⁻ cotransporter NBCn1 (Slc4a7) is increased in ErbB2-induced breast cancer tissue compared to normal, and disrupting NBCn1 expression delays ErbB2-induced breast cancer development [44]. However, the mechanisms of LRRC8A upregulation as well as the pathways involved in its tumor-promoting role were unexplored.

RNA modification is an important post-transcriptional regulation. By analyzing RNA-BisSeq data of HeLa cells [31], we found that LRRC8A mRNA may have m⁵C sites. RNA m⁵C modification is a widespread post-transcriptional RNA modification and participates in various cellular and physiological processes. NSUN2 is the main enzyme catalyzing m⁵C formation and plays an important role in the regulation of RNA fate, such as RNA stability, RNA processing, RNA export, and mRNA translation [15-20]. To explore the relationship among LRRC8A and m⁵C modification, we established RNA-seq in NSUN2 knockdown CC cells and found that LRRC8A was downregulated upon NSUN2 knockdown. Correlation analysis showed LRRC8A expression was positively correlated with NSUN2 expression in CC.

m⁵C methyltransferase NSUN6 was also demonstrated to mediate m⁵C methylation on mRNA [45]. However, no positive correlation between the mRNA levels of NSUN6 and LRRC8A in CC was observed (Fig. S6B), which is consistent with that only NSUN2 affects the global m⁵C level in mRNAs in HeLa cells [31]. MeRIP assays showed that LRRC8A mRNA was modified with m⁵C and NSUN2 depletion could decrease the level of m⁵C modification on LRRC8A mRNA. Also, RIP-seq in SiHa cells as well as RIP-PCR assays both confirmed that NSUN2 could specifically interact with LRRC8A mRNA. YBX1 is an m⁵C reader protein, and we found that YBX1 knockdown led to lower mRNA level of LRRC8A in CC cells. Since m⁵C modification was reported to be associated with regulating the stability of mRNA [16,17], we treated cells with actinomycin D and uncovered that knockdown of NSUN2 shortened the half-life of LRRC8A mRNA. These results indicate that NSUN2 promotes LRRC8A mRNA stability through m⁵C deposition and upregulates its expression in CC.

Notably, gene ontology analysis showed that differentially expressed genes in NSUN2-loss cells significantly enriched PI3K-Akt signaling pathway. PI3K/AKT pathway plays vital roles in various cellular processes and is involved in many diseases such as malignant tumors [37]. Several studies have reported that CC patients show abnormal activation of PI3K/AKT signaling, which may provide potential therapeutic targets of CC [38-40]. In the present study, we demonstrated that knockdown expression of NSUN2 and LRRC8A both could depress PI3K/AKT signaling pathway activation. Nevertheless, how this signaling pathway was activated in CC by NSUN2 and LRRC8A require more detailed and systematic studies. Apart from PI3K/AKT pathway, differentially expressed genes in NSUN2-depleted CC cells are enriched in multiple other oncogenic pathways, and NSUN2-deplete CC cells revealed the reduced global m⁵C level of mRNA. Thus, we explored the role of NSUN2 in CC cells. Results demonstrated that NSUN2 played a tumor-promoting role in CC. Depletion of NSUN2 significantly inhibited cell growth and metastasis, whereas ectopic expression of LRRC8A in NSUN2-depleted cells could largely rescue the tumor-suppressive effect of NSUN2 knockdown. Considering that HPV infection is an important causative factor of CC, we test whether NSUN2-LRRC8A regulation was associated with HPV infection. Results showed that the mRNA levels of NSUN2 and LRRC8A had no statistical difference in HPV+ CC compared with HPV- CC tissues according to analyzed two GEO datasets (Fig. S6C). Interestingly, recent research unveiled that high expression of the N6-methyladenosine methyl-

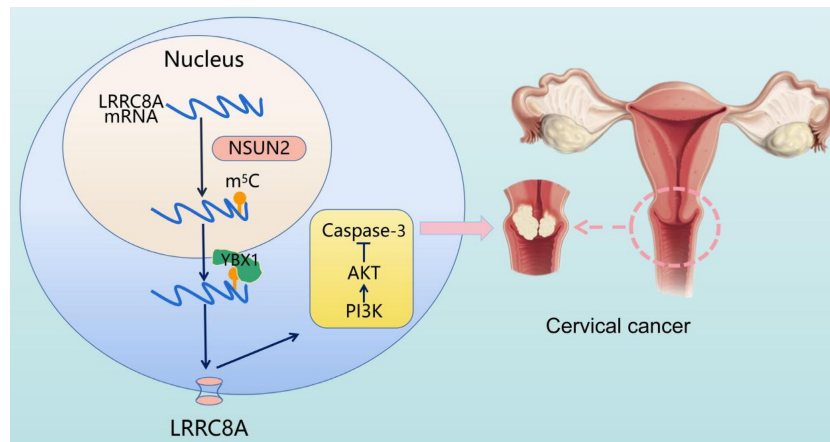


Figure 8. Schematic diagram illustrating the proposed mechanisms of m⁵C-mediated upregulation of LRRC8A in tumorigenesis of CC.

transferase METTL3 is associated with HPV status and CC patients' poor prognosis [46]. Thus, the relationship between RNA modifications including the m⁵C modification and HPV-infection needs more investigations.

In conclusion, elevated expression of LRRC8A in cervical cancer predicts a poor prognosis and promotes tumorigenesis *in vitro* and *in vivo*. The m⁵C modification enhances LRRC8A mRNA stability and upregulates its expression followed by PI3K/AKT signaling pathway activation in CC (Fig. 8). These findings contribute to our understanding the role of the NSUN2-m⁵C-LRRC8A axis in tumorigenesis of CC, and it might be a potential target for CC treatment.

Supplementary Material

Supplementary figures and table.

<https://www.ijbs.com/v19p0691s1.pdf>

Acknowledgements

This work was sponsored by the National Natural Science Foundation of China (32101164 and 82072886) and the Natural Science Foundation of Chongqing, China (CSTB2022NSCQ-MSX0897 and cstc2021jcyj-bshX0055).

Author contributions

Conceptualization, Ping Yi and Tao Liu; Data curation, Yanjie Chen; Formal analysis, Qinglv Wei and Jie Xu; Investigation, Yanjie Chen, Xinzhao Zuo, Xiaoyi Liu, Shiling Liu, Haocheng Wang, Qingya Luo, Yuya Wang and Hongyan Zhao; Project administration, Jing Xu, Tao Liu and Ping Yi; Supervision, Ping Yi and Tao Liu; Validation, Yanjie Chen; Writing-original draft, Yanjie Chen and Qinglv Wei; Writing-review & editing, Ping Yi and Tao Liu.

Competing Interests

The authors have declared that no competing interest exists.

References

- Sung H, Ferlay J, Siegel RL, Laversanne M, Soerjomataram I, Jemal A, Bray F. Global Cancer Statistics 2020: GLOBOCAN Estimates of Incidence and Mortality Worldwide for 36 Cancers in 185 Countries. *CA Cancer J Clin.* 2021, 71:209-249.
- Chen W, Zheng R, Baade P, Zhang S, Zeng H, Bray F, Jemal A, Yu X, He J. Cancer statistics in China, 2015. *CA: a cancer journal for clinicians.* 2016, 66:115-132.
- Suran M. Why US Cervical Cancer Survival Rates Haven't Improved for Decades. *JAMA.* 2022, 327:1943-1945.
- Allredge JK, Tewari KS. Clinical Trials of Antiangiogenesis Therapy in Recurrent/Persistent and Metastatic Cervical Cancer. *Oncologist.* 2016, 21:576.
- Lang F, Ritter M, Gamper N, Huber S, Fillon S, Tanneur V, Leppl-Wienhues A, Szabo I, Bulbins E. Cell volume in the regulation of cell proliferation and apoptotic cell death. *Cellular Physiology & Biochemistry.* 2000, 10:417-428.
- Lemonnier, L. Bcl-2-dependent modulation of swelling-activated Cl⁻ current and CIC-3 expression in human prostate cancer epithelial cells. *Cancer Research.* 2004, 64:4841-4848.
- Okada, Yasunobu. Volume expansion-sensing outward-rectifier Cl⁻ channel: Fresh start to the molecular identity. *American Journal of Physiology Cell Physiology* 1997.
- Akita T, Okada Y. Characteristics and roles of the volume-sensitive outwardly rectifying (VSOR) anion channel in the central nervous system. *Neuroscience.* 2014, 275:211-231.
- Syeda R, Qiu Z, Dubin AE, Murthy SE, Patapoutian A. LRRC8 Proteins Form Volume-Regulated Anion Channels that Sense Ionic Strength. *Cell.* 2016, 164:499-511.
- Qiu Z, Dubin A, Mathur J, Tu B, Reddy K, Miraglia L, Reinhardt J, Orth A, Patapoutian A. SWELL1, a Plasma Membrane Protein, Is an Essential Component of Volume-Regulated Anion Channel. *Cell.* 2014, 157:447-458.
- Rong X, Xw B, Cs A. Volume-regulated anion channel as a novel cancer therapeutic target. *International Journal of Biological Macromolecules.* 2020, 159:570-576.
- Kurashima K, Shiozaki A, Kudou M, Shimizu H, Arita T, Kosuga T, Konishi H, Komatsu S, Kubota T, Fujiwara H, et al. LRRC8A influences the growth of gastric cancer cells via the p53 signaling pathway. *Gastric Cancer.* 2021, 24:1063-1075.
- Lu P, Ding Q, Li X, Ji X, Li L, Fan Y, Xia Y, Tian D, Liu M. SWELL1 promotes cell growth and metastasis of hepatocellular carcinoma *in vitro* and *in vivo*. *EBioMedicine.* 2019, 48:100-116.
- Boccaletto P, Stefaniak F, Ray A, Cappannini A, Mukherjee S, Purta E, Kurkowska M, Shirvanizadeh N, Destefanis E, Groza P, et al. MODOMICS: a database of RNA modification pathways. 2021 update. *Nucleic acids research.* 2022, 50:D231-D235.
- Squires J, Patel H, Nousch M, Sibbritt T, Humphreys D, Parker B, Suter C, Preiss T. Widespread occurrence of 5-methylcytosine in human coding and non-coding RNA. *Nucleic acids research.* 2012, 40:5023-5033.
- Chen X, Li A, Sun B, Yang Y, Han Y, Yuan X, Chen R, Wei W, Liu Y, Gao C, et al. 5-methylcytosine promotes pathogenesis of bladder cancer through stabilizing mRNAs. *Nature cell biology.* 2019, 21:978-990.
- Su J, Wu G, Ye Y, Zhang J, Zeng L, Huang X, Zheng Y, Bai R, Zhuang L, Li M, et al. NSUN2-mediated RNA 5-methylcytosine promotes esophageal

- squamous cell carcinoma progression via LIN28B-dependent GRB2 mRNA stabilization. *Oncogene*. 2021.
18. Hussain S, Sajini A, Blanco S, Dietmann S, Lombard P, Sugimoto Y, Paramor M, Gleeson J, Odom D, Ule J, Frye M. NSUN2-mediated cytosine-5 methylation of vault noncoding RNA determines its processing into regulatory small RNAs. *Cell reports*. 2013; 4:255-261.
 19. Li Q, Li X, Tang H, Jiang B, Dou Y, Gorospe M, Wang W. NSUN2-Mediated m5C Methylation and METTL3/METTL14-Mediated m6A Methylation Cooperatively Enhance p21 Translation. *Journal of cellular biochemistry*. 2017; 118:2587-2598.
 20. Liu Y, Zhao Y, Wu R, Chen Y, Chen W, Liu Y, Luo Y, Huang C, Zeng B, Liao X, et al. mRNA m5C controls adipogenesis by promoting CDKN1A mRNA export and translation. *RNA biology*. 2021:1-11.
 21. Nombela P, Miguel-López B, Blanco S. The role of mA, mC and Ψ RNA modifications in cancer: Novel therapeutic opportunities. *Molecular cancer*. 2021; 20:18.
 22. Deneka, D., Sawicka, M., Lam, A. K. M., Paulino, C., and Dutzler, R. (2018). Structure of a volume-regulated anion channel of the LRRC8 family. *Nature* 558,254–259. doi: 10.1038/s41586-018-0134-y.
 23. Kasuya, G., Nakane, T., Yokoyama, T., Jia, Y., Inoue, M., Watanabe, K., et al. (2018). Cryo-EM structures of the human volume-regulated anion channel LRRC8. *Nat. Struct. Mol. Biol.* 25, 797–804. doi: 10.1038/s41594-018-0109-6.
 24. Kefauver, J. M., Saotome, K., Dubin, A. E., Pallesen, J., Cottrell, C. A., Cahalan, S. M., et al. (2018). Structure of the human volume regulated anion channel. *eLife* 7:e38461. doi: 10.7554/eLife.38461.
 25. Li T, Fan J, Wang B, Traugh N, Chen Q, Liu JS, Li B, Liu XS. TIMER: A Web Server for Comprehensive Analysis of Tumor-Infiltrating Immune Cells. *Cancer Research*. 2017; 77:e108.
 26. Li B, Severson E, Pignon J, Zhao H, Li T, Novak J, Jiang P, Shen H, Aster J, Rodig S, et al. Comprehensive analyses of tumor immunity: implications for cancer immunotherapy. *Genome biology*. 2016; 17:174.
 27. Yu M, Bardia A, Wittner B, Stott S, Smas M, Ting D, Isakoff S, Ciciliano J, Wells M, Shah A, et al. Circulating breast tumor cells exhibit dynamic changes in epithelial and mesenchymal composition. *Science (New York, NY)*. 2013; 339:580-584.
 28. Lu J, Xu F, Zhang J. Inhibition of angiotensin II-induced cerebrovascular smooth muscle cell proliferation by LRRC8A downregulation through suppressing PI3K/AKT activation. *Human cell*. 2019; 32:316-325.
 29. Kumar A, Xie L, Ta C, Hinton A, Gunasekar S, Minerath R, Shen K, Maurer J, Grueter C, Abel E, et al. SWELL1 regulates skeletal muscle cell size, intracellular signaling, adiposity and glucose metabolism. *eLife* 2020, 9
 30. Choi H, Ettinger N, Rohrbough J, Dikalova A, Nguyen HN, Lamb FS. LRRC8A channels support TNF α -induced superoxide production by Nox1 which is required for receptor endocytosis. *Free Radical Biology and Medicine*. 2016; 101:413-423.
 31. Yang X, Yang Y, Sun B, Chen Y, Xu J, Lai W, Li A, Wang X, Bhattarai D, Xiao W, et al. 5-methylcytosine promotes mRNA export - NSUN2 as the methyltransferase and ALYREF as an mC reader. *Cell research*. 2017; 27:606-625.
 32. A BHS, B CSDA, b SS, A IHL. Dual role of LRRC8A-containing transporters on cisplatin resistance in human ovarian cancer cells. *Journal of Inorganic Biochemistry*. 2016; 160:287-295.
 33. Platt C, Chou J, Houlihan P, Badran Y, Kumar L, Bainter W, Poliani P, Perez C, Dent S, Clapham D, et al. Leucine-rich repeat containing 8A (LRRC8A)-dependent volume-regulated anion channel activity is dispensable for T-cell development and function. *The Journal of allergy and clinical immunology*. 2017; 140:1651-1659.e1651.
 34. Lahey LJ, Mardjuki RE, Wen X, Hess GT, Li L. LRRC8A:C/E Heteromeric Channels Are Ubiquitous Transporters of cGAMP. *Molecular Cell*. 2020; 80:578-591.e575.
 35. Zhou C, Chen X, Planells-Cases R, Chu J, Wang L, Cao L, Li Z, López-Cayueño K, Xie Y, Ye S, et al. Transfer of cGAMP into Bystander Cells via LRRC8 Volume-Regulated Anion Channels Augments STING-Mediated Interferon Responses and Anti-viral Immunity. *Immunity*. 2020; 52:767-781.e766.
 36. Zhang H, Deng Z, Zhang D, Li H, Zhang L, Niu J, Zuo W, Fu R, Fan L, Ye J, She J. High expression of leucine-rich repeat-containing 8A is indicative of a worse outcome of colon cancer patients by enhancing cancer cell growth and metastasis. *Oncology reports*. 2018; 40:1275-1286.
 37. Vivanco I, Sawyers CL. The phosphatidylinositol 3-Kinase AKT pathway in human cancer. *Nature Reviews Cancer*. 2002; 2:489-501.
 38. Che Y, Li Y, Zheng F, Zou K, Li Z, Chen M, Hu S, Tian C, Yu W, Guo W, et al. TRIP4 promotes tumor growth and metastasis and regulates radiosensitivity of cervical cancer by activating MAPK, PI3K/AKT, and hTERT signaling. *Cancer letters*. 2019; 452:1-13.
 39. Qian M, Xiang L, Kang Z, Wu Z, Li X. Genetic and Methylation-Induced Loss of miR-181a2/181b2 within chr9q33.3 Facilitates Tumor Growth of Cervical Cancer through the PIK3R3/Akt/FoxO Signaling Pathway. *Clinical Cancer Research An Official Journal of the American Association for Cancer Research*. 2017; 23:575.
 40. Yang W, Chen M, Xu R, Zheng P. PRDM4 inhibits cell proliferation and tumorigenesis by inactivating the PI3K/AKT signaling pathway through targeting of PTEN in cervical carcinoma. *Oncogene*. 2021; 40:3318-3330.
 41. Bafaro E, Liu Y, Xu Y, Dempski R. The emerging role of zinc transporters in cellular homeostasis and cancer. *Signal transduction and targeted therapy*. 2017; 2.
 42. Cheng X, Wang J, Liu C, Jiang T, Yang N, Liu D, Zhao H, Xu Z. Zinc transporter SLC39A13/ZIP13 facilitates the metastasis of human ovarian cancer cells via activating Src/FAK signaling pathway. *Journal of experimental & clinical cancer research: CR* 2021, 40:199.
 43. Samimi G, Safaei R, Katano K, Holzer A, Rochdi M, Tomioka M, Goodman M, Howell S. Increased expression of the copper efflux transporter ATP7A mediates resistance to cisplatin, carboplatin, and oxaliplatin in ovarian cancer cells. *Clinical cancer research: an official journal of the American Association for Cancer Research*. 2004; 10(14):4661-4669.
 44. Toft N, Axelsen T, Pedersen H, Mele M, Burton M, Balling E, Johansen T, Thomassen M, Christiansen P, Boedtker E. Acid-base transporters and pH dynamics in human breast carcinomas predict proliferative activity, metastasis, and survival. *eLife*. 2021; 10.
 45. Selmi T, Hussain S, Dietmann S, Heiss M, Borland K, Flad S, Carter JM, Dennison R, Huang YL, Kellner S et al: Sequence- and structure-specific cytosine-5 mRNA methylation by NSUN6. *Nucleic Acids Res* 2021, 49(2):1006-1022.
 46. Yu R, Wei Y, He C, Zhou P, Yang H, Deng C, Liu R, Wu P, Gao Q, Cao C: Integrative Analyses of m6A Regulators Identify that METTL3 is Associated with HPV Status and Immunosuppressive Microenvironment in HPV-related Cancers. *Int J Biol Sci* 2022, 18(9):3874-3887.